The ISME Journal (2011) 5, 1759–1770

www.nature.com/ismej

ORIGINAL ARTICLE

Linking phytoplankton community composition to seasonal changes in *f*-ratio

Bess B Ward[1,2], Andrew P Rees[1], Paul J Somerfield[1] and Ian Joint[1]
[1]*Marine Life Support Systems, Plymouth Marine Laboratory, Plymouth, Devon, UK and* [2]*Department of Geosciences, Princeton University, Princeton, NJ, USA*

Seasonal changes in nitrogen assimilation have been studied in the western English Channel by sampling at approximately weekly intervals for 12 months. Nitrate concentrations showed strong seasonal variations. Available nitrogen in the winter was dominated by nitrate but this was close to limit of detection from May to September, after the spring phytoplankton bloom. The ^{15}N uptake experiments showed that nitrate was the nitrogen source for the spring phytoplankton bloom but regenerated nitrogen supported phytoplankton productivity throughout the summer. The average annual *f*-ratio was 0.35, which demonstrated the importance of ammonia regeneration in this dynamic temperate region. Nitrogen uptake rate measurements were related to the phytoplankton responsible by assessing the relative abundance of nitrate reductase (*NR*) genes and the expression of *NR* among eukaryotic phytoplankton. Strong signals were detected from *NR* sequences that are not associated with known phylotypes or cultures. *NR* sequences from the diatom *Phaeodactylum tricornutum* were highly represented in gene abundance and expression, and were significantly correlated with *f*-ratio. The results demonstrate that analysis of functional genes provides additional information, and may be able to give better indications of which phytoplankton species are responsible for the observed seasonal changes in *f*-ratio than microscopic phytoplankton identification.
The ISME Journal (2011) **5,** 1759–1770; doi:10.1038/ismej.2011.50; published online 5 May 2011
Subject Category: geomicrobiology and microbial contributions to geochemical cycles
Keywords: *f*-ratio; seasonal variation; nitrate reductase gene expression; microarrays

Introduction

The western English Channel is one of the best-studied marine regions, with a long time series of measurements. Research was initiated in the late nineteenth century as an investigation to explain variability in the fishery (Southward *et al.*, 2005). Among the earliest factors to be studied were temperature and a variety of chemical measurements. For example, the first determination of phosphate concentration was made in 1916 (Matthews, 1917) and frequent, regular measurements began in 1923. The studies from the English Channel in this period laid the basis for much subsequent understanding of chemical oceanography, including observations on nitrate to phosphate ratio in the English Channel (Cooper, 1937)—observations that were to be collated from a range of geographical provinces to form the Redfield ratio hypothesis (Redfield *et al.*, 1963).

Nutrient measurements have been a particularly important part of studies to understand productivity in the English Channel. Russell (1936) made an early link between phosphate concentration and pelagic biology when he noted a correspondence between the abundance of young fish and phosphate concentration. Initially concerned with interannual variation, Russell showed that for the period 1923–1935, there was good correspondence between mean winter phosphate maxima and young fish abundance (Russell, 1936). Later research focused on these winter concentrations of phosphate (that is, the yearly maxima), which were thought to be an important driver of long-term fluctuations in the Channel ecosystem (Russell *et al.*, 1971; Southward *et al.*, 2005), fluctuations that were referred to as the Russell Cycle (Cushing and Dickson, 1976). Later workers found that temperature was a major determinant of the timing of maximum fish abundance (Genner *et al.*, 2010). A number of variations in species abundance were observed between the 1920s and the 1980s, including a decline in abundance of zooplankton, a change of the plankton community from that characterized by the chaetognath *Sagitta elegans* to one characterized by the more neritic species *Sagitta setosa* and the failure of the herring fishery off Plymouth in 1936 (Southward *et al.*, 2005).

Throughout this long period, phosphate concentrations were measured routinely and frequently in

Correspondence: BB Ward, Marine Life Support Systems, Plymouth Marine Laboratory, Prospect Place, The Hoe, Plymouth, Devon PL1 3DH, UK.
E-mail: bbw@princeton.edu
Received 4 November 2010; revised 11 March 2011; accepted 24 March 2011; published online 5 May 2011

every season and the methodologies were adapted and improved (Joint *et al.*, 1997). The time series of dissolved inorganic nitrogen concentrations in the western English Channel is less complete, partly because a reliable method of nitrate analysis was developed much later than that for phosphate. Although interannual variations in nutrient concentrations have been described for the region (Jordan and Joint, 1998), the processes that influence the nitrogen cycle, and result in season changes in concentration, have been less thoroughly investigated.

In this paper, we describe a seasonal study of phytoplankton uptake of nitrate and ammonium in the context of changes in nutrient concentration. These uptake measurements are linked to phytoplankton community structure through the use of functional gene microarrays targeted to eukaryotic phytoplankton nitrate reductase (*NR*) genes. All measurements are placed within the context of a large body of data on physics, chemistry and biology of the English Channel (Harris, 2010; http://www.westernchannelobservatory.org.uk/). The aim of the study is to provide better understanding of how changes in community composition and gene expression of the phytoplankton assemblage might correlate with activity and biogeochemical cycles. It is hoped that this will improve parameterization for models involved in assimilating data derived from satellite remote sensing (Smyth *et al.*, 2010).

Materials and methods

Study site and sample collection

At approximately weekly intervals between March 2004 and February 2005, water samples were collected from Station L4 (Harris, 2010) in the English Channel (50°15′N, 4°13′W). The Western Channel has been studied for more than 100 years, with a large contextual data set of physical, chemical and biological data (Southward *et al.*, 2005; Smyth *et al.*, 2010) within which to place new measurements. Station L4 is typical of UK temperate coastal waters, and is largely composed of central English Channel water with, occasionally, influences of river run-off (Siddorn *et al.*, 2003, Rees *et al.*, 2009). The station is now part of a long-term ocean observatory, the Western English Channel (http://www.westernchannelobservatory.org.uk/).

Water samples were taken by pump from just below the sea surface (~1 m depth) as part of the standard sampling protocol and transported to the laboratory in 20 l carboys. Immediately upon return to the laboratory (~2–4 h after sampling), the water was processed for different measurements. Ammonium and nitrate uptake incubations were initiated immediately; nutrient concentrations were measured within 2 h of the water arriving in the laboratory; samples for molecular and microarray analyses were filtered within 2 h onto Sterivex (Millipore, Billerica, MA, USA) filter capsules (4–6 litre per capsule) and frozen at −80 °C. Approximately 20 min was required to filter 4–6 litre of water and two capsules were handled simultaneously.

Nutrients

Micromolar (μmol l^{-1}) nitrate, nitrite, silicate and phosphate concentrations were measured on a 5-channel Technicon segmented flow colorimetric autoanalyzer (Bran + Luebbe, AAII, Seal Analytical, Hampshire, UK) with detection limits of 0.1 μmol l^{-1} for all channels. Further details may be found elsewhere (Woodward and Rees, 2001). Ammonium concentration was measured by the orthophthaldialdehyde method (Holmes *et al.*, 1999). As with all fluorometric determinations, there are challenges in both establishing a baseline and obtaining ammonia-free water. In addition, the fluorescence of orthophthaldialdehyde method is different in distilled water and sea water. In this study, low-ammonia sea water for blank determination was obtained by exploiting the diffusion of ammonia through a polytetrafluoroethylene membrane (Gibb *et al.*, 1995). Polytetrafluoroethylene tubing was filled with concentrated H_2SO_4, sealed and immersed in 1 litre filtered sea water, taking care to ensure that no acid was introduced into the sea water. After 24 h, the ammonia concentration in the sea water was significantly reduced as ammonia, after diffusing through the polytetrafluoroethylene, was scavenged by the acid. For each determination of ammonia in sea water, standard curves were constructed from ammonia additions to this low-ammonia sea water; standard additions of known ammonia concentrations were also added to each environmental sample to check the fluorometric response of the orthophthaldialdehyde method.

Phytoplankton counts and pigments

Paired water-bottle samples were collected from a depth of 1 m and preserved with 2% Lugol's iodine solution (Throndsen, 1978) and 4% buffered formaldehyde. Between 10 and 100 ml of sample, depending on cell density, were settled for >48 h and all phytoplankton cells were identified where possible to species level and enumerated (Widdicombe *et al.*, 2010). Cell volumes were calculated according to the equations of Kovala and Larrance (1966) and converted to carbon (Menden-Deuer and Lessard, 2000). Pigments were extracted from filtered phytoplankton and analyzed by high-performance liquid chromatography as previously described (Llewellyn *et al.*, 2005).

^{15}N-nitrate and -ammonium uptake rates

Aliquots from the 20 l carboys were measured into six 250 ml bottles; three received 0.5 μmol l^{-1} $^{15}NO_3$ and three received 0.05 μmol l^{-1} $^{15}NH_4$ final concentrations. Experiments were done in a large

temperature-controlled tank of sea water in a constant temperature laboratory that was maintained at ambient seawater temperature, as described by Joint and Jordan (2008). Photon flux similar to sunlight was achieved using three quartz halogen lamps (Osram Power Star, 150 W, Munich, Germany); heating was not a problem because the samples were incubated in a large volume of water in the water tank (1000 l). Throughout the annual study, samples were incubated 0.5 m from the light source and all experiments received the same photon flux—550 μmol quanta $m^{-2} s^{-1}$.

For each tracer addition, two bottles were incubated in the light and one in the dark. As the aim of the study was to investigate nitrogen uptake by phytoplankton associated with photosynthetic carbon fixation, rather than by the whole microbial assemblage, uptake rates measured in the dark incubations have been subtracted from those in the light, to give an estimate of the phytoplankton-specific nitrogen assimilation. After 3 h, the entire contents of each bottle were filtered onto 25 mm GF/F filters and dried. The particulate carbon, particulate nitrogen (PN) and $^{15/14}N$ ratio of the PN were determined using an isotope ratio mass spectrometer (Europa 20/20, SerCon, Cheshire, UK). Uptake rates were calculated using the equations of Dugdale and Goering (Dugdale and Goering, 1967) assuming constant substrate atom-% over the short incubation.

Probe and array design

The phytoarray is a functional gene microarray containing probes representing functional genes from major eukaryotic phytoplankton groups. Oligonucleotide probes representing *NR* genes were selected from sequences contained in the public databases (Genbank). The phytoarray is an archetype array, in which each group of similar sequences is represented by a single archetype probe, which differs from all other archetypes by at least 15% sequence identity, chosen to represent the relevant database (for example, all marine algae) while minimizing overlap between probes. The probe selection method (Bulow *et al.*, 2008), complete list of probes, probe sequences and database sequences used to design the archetypes have been described previously (Ward, 2008). The phytoarray contained 16 *NR* probes, which include 8 diatom probes, 4 chlorophyte probes and 3 *NR* probes representing sequences of unknown affiliation. Arrays contained two sets of replicate blocks such that each specific probe was represented in two blocks, providing eight replicate features in each array. Two to eight features in each block were spotted with equimolar mixtures of all gene-specific probes present on the array. These MIXALL probes were used for signal normalization (see below).

The probes were manufactured as 90-bp oligonucleotides, each containing the 70-mer probe sequence described above plus a 20-mer universal reference sequence (5′-GATCCCCGGGAATTGCCA TG-3′). The presence of the same reference sequence in each feature was intended for use in quantification and normalization (Dudley *et al.*, 2002). The 90-mer oligo probes (Integrated DNA Technologies, Coralville, IA, USA) were adjusted to a concentration of 0.05 μg $μl^{-1}$ in 50% dimethylsulfoxide and were spotted on CMT-GAPS amino silane-coated glass slides (Corning Inc., Corning, NY, USA) using a robotic style arrayer (DeRisi *et al.*, 1996), in the Princeton University Molecular Biology Array Facility. After printing, the slides were baked at 80 °C for 3 h and stored in the dark at room temperature under slight vacuum.

DNA and RNA purification

Particulate material from sea water collected on Sterivex filters was lysed and the DNA extracted using a slight modification of the Gentra PureGene tissue protocol (Qiagen, Valencia, CA, USA). Volumes of the various buffers were doubled in order to improve recovery from the filter capsules and lysis was performed inside the filter capsule. The resulting DNA was ready for PCR without further purification and was stored at −20 °C.

RNA was recovered from the sterivex filter capsules using the RNAqueous kit from Ambion (Applied Biosystems, Foster City, CA, USA) by doubling the buffer volumes and carrying out the lysis step inside the filter capsules. Immediately following elution of the RNA from the spin column, it was transcribed using Superscript III from Invitrogen (Carlsbad, CA, USA), using either oligo-d(T) or random hexamer primers. The remaining RNA and complementary DNA (cDNA) was stored at −80 °C until further use.

PCR amplification

To produce PCR targets for hybridization with the array, DNA was amplified with gene-specific primers using the nested PCR approach (Allen *et al.*, 2005). The NR primers amplify *NR* genes from all diatoms tested so far, several other algal groups in culture and field samples (Bhadury and Ward, 2009), but do not amplify *NR* genes from chlorophytes or prokaryotes (Allen *et al.*, 2005). Primers NRPt907F and NRPt2325R were used for the first (outer) round of *NR* amplification, and NRPt1000F and NRPt1389 for inner amplification. The second round of amplification used 1–5 μl of the outer reaction as a template with the same PCR protocol.

Target preparation

Hybridization targets were produced from PCR products. The product obtained from the standard PCR above was labeled by random priming using Klenow fragment and random octomers supplied in the BioPrime labeling kit (Invitrogen). The standard

dNTP mixture was replaced with a mixture of 1.2 mM dNTP containing A/C/G/T/U in the ratio of 6:6:6:2:4, in which the U was the amino-allyl-modified base dUTPaa. Parallel reactions were pooled and again cleaned with Qiaquick columns (Qiagen), and the eluted dUTPaa-labeled DNA was dried under vacuum and stored as a dry pellet at −20 °C.

The dUTPaa-labeled fragments (200–2000 ng) were labeled with Cy3 (Cy3 mono-functional NHS ester; GE Healthcare Bio-Sciences Corp., Piscataway, NJ, USA) as previously described (Ward, 2008). Immediately before hybridization, the target was dissolved in water using a volume calculated to provide a convenient addition to the hybridization chamber. The concentration of target was computed by measuring the DNA concentration and Cy3 concentration of the Qiaquick eluate before the last drying step. DNA concentration was quantified using the PicoGreen kit (Invitrogen) and a JASCO fluorometer (Essex, UK).

Hybridization, scanning and quantification of array data

Cy3-labeled target (200 ng for arrays using targets produced by PCR) plus 100 pmol of the reverse Cy5-labeled 20-mer reference oligonucleotide in a total volume of 200 μl was pipetted into the gasket area of the coverslip (Agilent Technologies, Santa Clara, CA, USA). The slides were placed inside hybridization chambers (Agilent), and rotated at 8–12 cycles per min at 55 °C for ∼16 h. After hybridization, the coverslip was removed and the slides washed in three successive 10–20 min washes at room temperature (wash 1 = 1 × SSC (salt, sodium citrate solution), 0.05% SDS (sodium dodecyl sulfate); wash 2 = 0.1 × SSC, 0.05% SDS; wash 3 = 0.1 × SSC). After the last wash, the slide was dried by centrifugation. The dried slides were stored at room temperature in the dark and scanned with an Axon 4200 laser scanner (Molecular Devices, Sunnyvale, CA, USA).

The scanner determined Cy3 (green) and Cy5 (red) fluorescence for each spot in the array using Gene Pix Pro 6.0 (Axon Instruments). The fluorescence data were transferred to Excel spreadsheets for manipulation and quantification and filtered for quality control as follows. The average background value for all spots was computed and spots with backgrounds exceeding the average value by 2 s.d. were removed. This usually involved removing 1 or 2 features (obvious printing problems or slide blemishes) from each array whose backgrounds exceeded the average by ∼1000 ×. The average and s.d. of the background for all dots were recomputed. Spots whose red or green fluorescence did not exceed the background value by 1 s.d. were not considered to contain significant signal and were removed from further calculations. For spots that passed the background filter cutoff, the Cy3/Cy5 ratio was computed and an average and s.d. of the ratio were computed for each set of replicate features. The average Cy3/Cy5 ratio for replicate features was considered significant if the *T*-statistic (Wurmbach *et al.*, 2003) exceeded 3 (it usually exceeded 5).

The main source of signal variability was between replicate blocks, whereas within-block replication was excellent (T often >20 for $n=4$ to 5). Both arrays included features that contained constructed mixtures (MIXALL probes) of the specific probes in each block, and these provided excellent correction for between- and within-block variability in hybridization. The average Cy3/Cy5 ratio for the MIXALLs in each block was computed and used to correct for differences in hybridization intensity between duplicate blocks on the same array. The average coefficient of variation (s.d. as a percent of the mean) for replicate Cy3/Cy5 ratios within arrays was 16%, the highest variance being associated with smallest ratios. For each target, duplicate arrays were hybridized and the average relative fluorescence ratio (RFR) for each archetype—a measure of the hybridization signal—was used in subsequent analyses. Average RFR values for replicate arrays varied by 8–15%, as reported previously in an extensive investigation of the reproducibility of this array format (Ward, 2008).

All of the original array files are available at GEO (Gene Expression Omnibus; http://www.ncbi.nlm.nih.gov/projects/geo/) at NCBI (National Center for Biotechnology Information) under GEO accession number GSE27998.

Statistical analyses

Biogeochemical, hydrographic and microarray hybridization data were subjected to multivariate statistical analyses using PRIMER (Clarke and Warwick, 2001; Clarke and Gorley, 2006) and R (http://cran.r-project.org/). Two-dimensional non-metric multidimensional scaling was used to cluster the archetypes according to their temporal patterns, whereas principal components analysis was used to investigate relationships among archetypes and chemical and physical variables. Physical, chemical and rate data were log transformed before using PRIMER, and *f*-ratio and array RFR values were arcsin transformed before performing regression and correlation analysis with R. When results are stated as significant, it means that the relationship was significant at the level of $P \leqslant 0.05$.

Results

Nutrients concentrations over the annual cycle

During the period of this study, temperature varied from a minimum of 9.0 °C in January to a maximum of 18.8 °C in late August. Salinity was relatively invariant at 35.11 ± 0.24 over the year; the lowest salinities were associated with late autumn storms

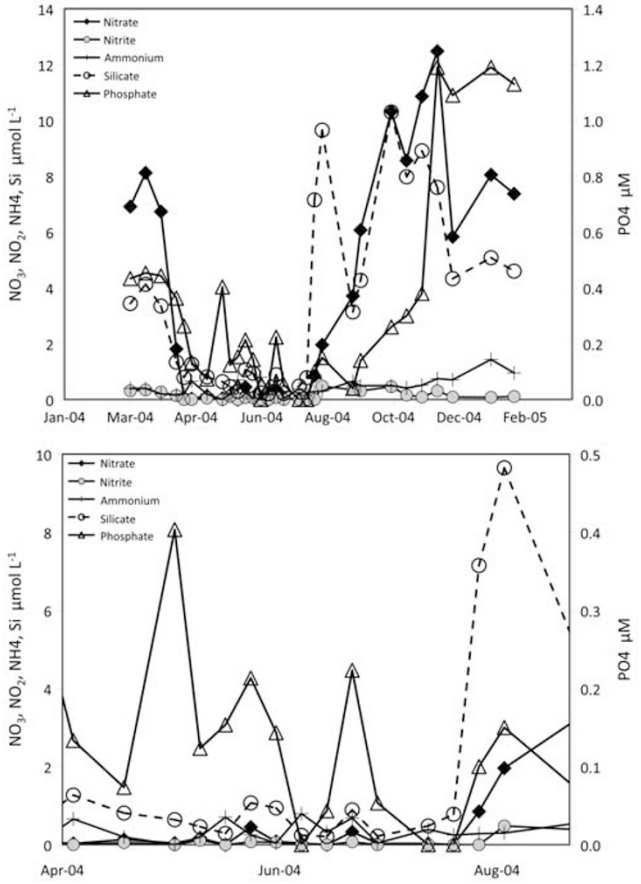

Figure 1 Concentrations ($\mu mol\,l^{-1}$) of nitrate, nitrite, ammonium, silicate and phosphate (right axis) measured in the surface waters at L4 during the study. (Bottom panel) Expanded scale for summer months.

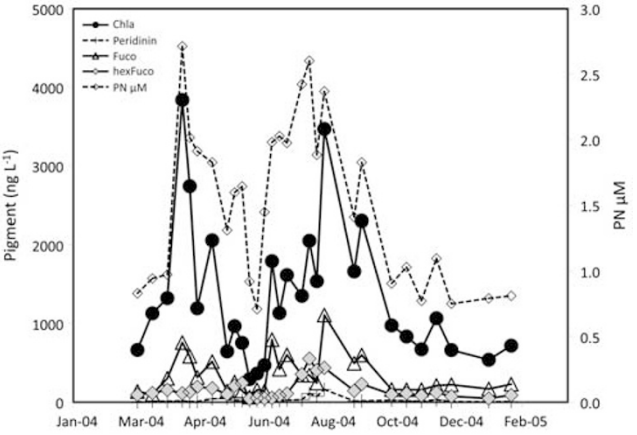

Figure 2 Chlorophyll *a*, peridinin, fucoxanthin and hexfucoxanthin concentrations ($ng\,l^{-1}$) determined by high-performance liquid chromatography (HPLC) analysis. Right axis is the organic PN concentration determined by mass spectroscopy in the ^{15}N uptake experiments.

when there was a significant increase in run-off. Nutrient concentrations in the surface water at Station L4 underwent a typical seasonal cycle (Figure 1). All three major nutrients (N, P, and Si) were present at high concentrations in winter (December–March), decreased in spring (late March–April) as a consequence of the increase in phytoplankton during the spring bloom, remained at consistently low levels throughout the summer (May–July/August) before increasing again in late fall (August–November). There were a few sporadic increases in phosphate or silicate—but not nitrate—during the summer, in which either nutrient was present at relatively high concentrations at a single time point. The molar ratio of nitrate (N) to silicate (Si) varied from 0.02 to 2 (mean $= 0.83 \pm 0.72$). Nitrate concentrations were higher than silicate in the winter, but the ratio was <1 in summer, suggesting potential nitrate limitation of diatom growth. The nitrate/phosphate ratio was very close to 16 in January of 2004, and then varied widely from 0.1 to >90 and leveled out at ~ 6 by the end of the year. Nitrate, nitrite and silicate were all positively correlated with each other and with salinity, but were negatively correlated with temperature, suggesting Atlantic Ocean rather than freshwater river sources for the nutrients. Phosphate concentration was weakly correlated with silicate concentration but was not related to any other nutrients or physical/chemical variables (Supplementary Table 1).

Phytoplankton community composition

The seasonal patterns of phytoplankton species composition and photosynthetic pigments have been described previously for this site (Rodriguez *et al.*, 2000; Llewellyn *et al.*, 2005). Here we emphasize the diatom component because this group was best represented in the microarray analysis. Although highly variable on a weekly basis, the annual cycle usually includes two major blooms, to which both diatoms and flagellates contribute major portions of the biomass. In 2004, chlorophyll concentration indicated two bloom periods (Figure 2), the first from mid-April to mid-May, and the second, of slightly lower maximum chlorophyll concentration but longer duration, from early July to late September. Fucoxanthin concentration—a marker for diatoms—followed a very similar temporal pattern and was highly correlated with chlorophyll concentration ($R^2 = 0.761$, $P \ll 0.001$), as reported previously for a 3-year data set at this station (Llewellyn *et al.*, 2005). Neither chlorophyll *a* nor fucoxanthin concentrations were correlated with total phytoplankton carbon, diatom carbon or nitrate concentration. As reported by Llewellyn *et al.* (2005), the relationship between chlorophyll *a* and total phytoplankton carbon was a significant positive correlation ($R^2 = 0.74$, $P = 0.0003$) for samples in which the chlorophyll *a*/total phytoplankton carbon ratio was >0.04, but was more variable for warm season samples when the ratio was lower (<0.04) and more variable. Both

chlorophyll *a* ($R^2 = 0.59$, $P \ll 0.001$) and fucoxanthin ($R^2 = 0.53$, $P \ll 0.001$) concentration were positively correlated with PN concentration, as measured by mass spectrometry in the ^{15}N uptake experiments. Total carbon estimated from phytoplankton counts and PN measured by mass spectrometry were not well correlated and suggested an average carbon/nitrogen ratio of 2.4, well below that usually reported for biomass. The total carbon/nitrogen ratio averaged over 2004 from the WCO (http://www.westernchannelobservatory.org.uk/) was 8.1, much closer to the usual average for biomass, and suggesting slight N limitation.

Correlations between fucoxanthin and chlorophyll *a* concentrations imply that diatoms were major contributors to the overall biomass represented by chlorophyll throughout the year. The correlations between both chlorophyll *a* and fucoxanthin and PN again suggest that diatoms were major contributors to the live biomass, and that most of the PN was associated with live phytoplankton rather than non-living material. Lack of significant correlations between pigments other than chlorophyll *a* and fucoxanthin with PN and particulate carbon estimated from the microscopy counts suggests that these estimates did not reflect live biomass accurately. Additionally, fucoxanthin and PN were positively correlated with the rate of nitrate assimilation (see below; Supplementary Table 1), consistent with a major role for diatoms in assimilating nitrate and driving new production in this region.

Several diatom species achieved their maximum abundance (as determined by microscope counts) for the year in the week of, or the week following, the large silicate injection in late August. Presumably the silicate injection and maximum nitrate assimilation rates measured on 25 August led to the biomass accumulation within the next few days, which we captured in the weekly sampling on 31 August. Several of the same species contributed to the smaller maxima in diatom carbon abundance in May, June and July. These species, including *Chaetoceros socialis*, *Guinardia delicatula*, *Leptocylindrus danicus*, *Nitzschia closterium*, *Pseudonitzschia* spp., *Rhizosolenia stolterfothii* and other *Rhizosolenia* spp., and several *Thalassiosira* species, were the major components of the diatom assemblage in terms of cell carbon over the annual period.

Nitrate and ammonium uptake rates

Nitrate and ammonium uptake rates both varied on time scales of several weeks (Figure 3). The first spring maximum in nitrate uptake preceded the first maximum in ammonium uptake rate, and was associated with the spring maximum in chlorophyll concentration. A second brief maximum in uptake rates of both N sources occurred during a minimum in the chlorophyll concentrations, but the highest

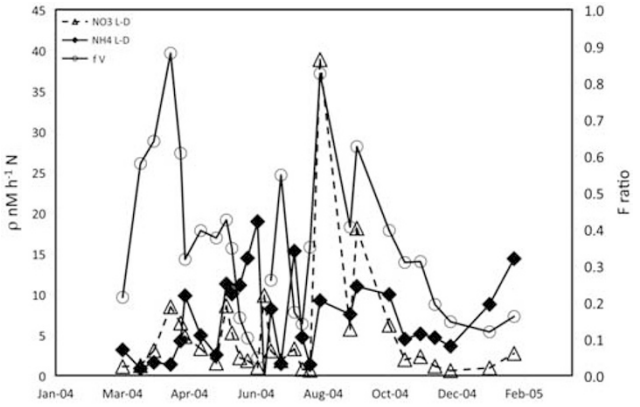

Figure 3 Uptake rates (ρ) of nitrate and ammonium (light minus dark) determined in ^{15}N tracer experiments and *f*-ratio.

nitrate uptake rates occurred at the time of the late August chlorophyll maximum. The peak nitrate uptake rate on 25 August coincided with a large silicate injection that was not accompanied by an increase in nitrate concentration, suggesting that phytoplankton assimilation of nitrate maintained low concentrations. The second highest nitrate assimilation measured over the year was recorded in late September, when both nitrate and silicate concentrations were at or near their fall maxima.

Specific uptake rates (V) for nitrate and ammonium varied in parallel to their total uptake rates (ρ). These rates suggest maximum growth rates (assuming a 12 h light period) in terms of nitrogen of <0.5 per day (0.26 per day for NH_4^+ on 21 June and 0.21 per day for NO_3^- on 25 August). The average growth rates, however, were much lower, 0.037 per day $\pm$ 0.042 for NO_3^- and 0.071 per day $\pm$ 0.062 for NH_4^+. These rates are well below the maximum predicted for nutrient replete growth at the observed temperatures (Eppley, 1972), but many of the species enumerated from these samples have optimal growth temperatures higher than those observed at L4. Thus, both temperature and nutrient availability could be factors controlling the growth rate and specific uptake rates of the overall assemblage. The *f*-ratio, computed on the basis of light minus dark uptake rates, ranged from 0.05 (late June) to >0.8 (mid-April, late August). When calculated as a time-averaged value over the period of the study, the annual *f*-ratio was 0.35, indicating the importance of regenerated production in this temperate coastal zone.

Correlation-based principal components analysis of DIN concentrations and uptake rates across all months identified important temporal patterns (Figure 4). The first principal component essentially contrasts dates with high uptake rates with dates with high levels of nitrate and nitrite, and explains 33.6% of the variance. The second principal component, explaining a further 26.6% of the variance, separates dates with high *f*-ratio and NO_3^-

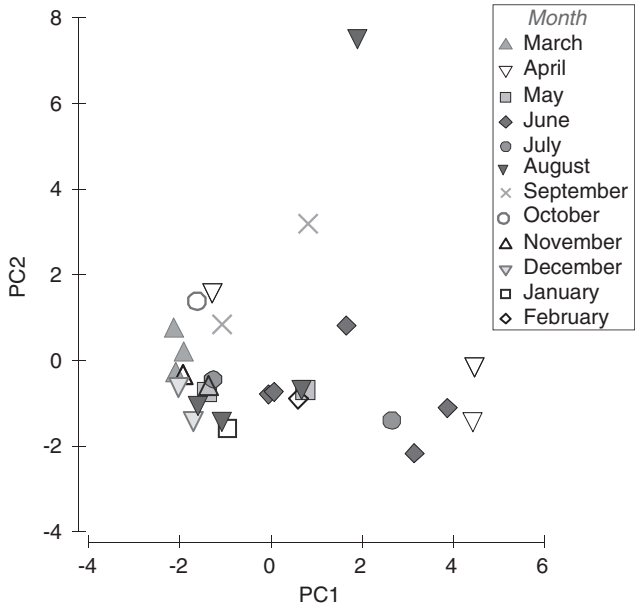

Figure 4 Principal components analysis based on a correlation matrix of chemical (nutrients), physical (temperature, salinity) and biological (uptake rates, *f*-ratio, pigments) factors at each sample date.

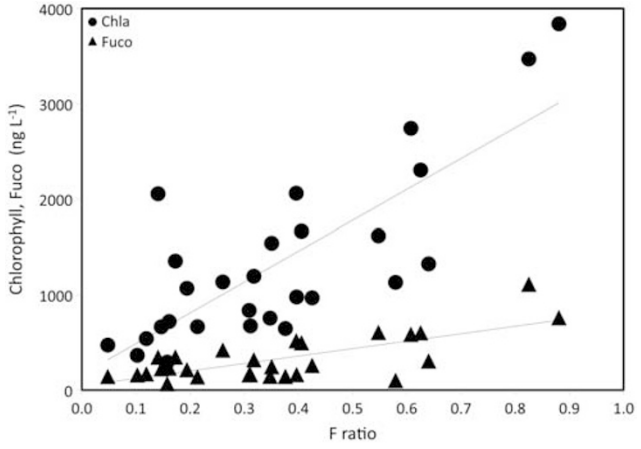

Figure 5 Chlorophyll *a* concentration (Chl) and fucoxanthin (Fuco) concentration plotted against *f*-ratio. Chl (ng l^{-1}) = 3215.8 (*f*-ratio) + 164.13, $R^2 = 0.6023$, $P < 0.0001$; Fuco (ng l^{-1}) = 784 (*f*-ratio) + 41.92, $R^2 = 0.5056$, $P < 0.0001$.

uptake in the light from dates with high NO_3^- concentration. For example, the two dates in late April (late spring bloom: low NO_3^- concentration) clustered opposite all three March dates and the early April date (early spring: high NO_3^- concentration, low NO_3^- assimilation rates). The five dates in June were not clustered coherently, which is consistent with the great variability observed in N uptake and N concentrations over that month (Figures 1 and 3). Most significantly, the late August date (very high *f*-ratio and high N uptake rate) was well separated from all other dates in Figure 4. This is consistent with the high NO_3^- uptake measure-

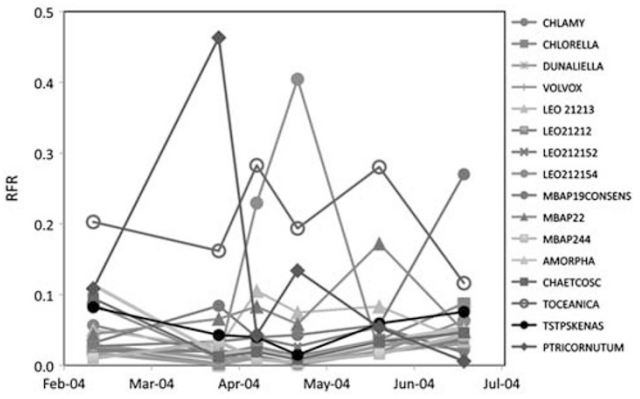

Figure 6 RFR for DNA hybridization signals from each *NR* archetype at six dates. Errors for individual points not shown for clarity; see Materials and methods.

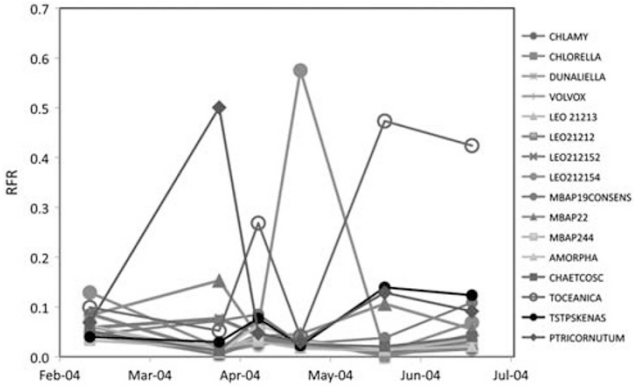

Figure 7 RFR for cDNA hybridization signals from each *NR* archetype at six dates. Errors for individual points not shown for clarity; see Materials and methods.

ments and high *f*-ratio measured in late August. The large temporal signal in most environmental variables (Figure 1) probably explains the lack of simple correlations between temporally contiguous samples and single physical/chemical variables. The *f*-ratio was positively correlated with both chlorophyll *a* ($R^2 = 0.47$, $P \ll 0.001$) and fucoxanthin ($R^2 = 0.25$, $P \ll 0.006$) concentrations (Figure 5). The highest *f*-ratios coincided with the spring and late summer maxima in nitrate uptake rates and pigment concentrations.

NR *archetype relative abundance and gene expression*
Array analysis was performed on samples from six dates, all before the August silicate injection. The strongest hybridization signals (RFR) determined from *NR* PCR targets prepared from DNA indicated the presence of archetypes representing *Phaeodactylum tricornutum*, *Thalassiosira oceanica* and two archetypes representing unknown *NR* sequences (Figure 6). The two unknown archetypes, LEO212154 and MBAP19CONSENS, represent multiple similar sequences originally derived from New Jersey coastal waters (both archetypes) and

Monterey Bay (MBAP19CONSENS) that were available at the time this probe set was designed. These four high signal probes all showed different temporal patterns.

Three of the archetypes that yielded high DNA RFR were also large RFR signals in the PCR targets prepared from cDNA. Of the four high DNA RFR archetypes, only MBAP19CONSENS cDNA was not significantly different from the rest of the archetypes, which showed generally lower and less variable signals (Figure 7).

Low hybridization signals were observed for the archetype probes representing chlorophyte algal *NR* genes. The *NR* PCR primers used here were designed to target diatoms and they amplify known green algal sequences not at all or with very low efficiency. The RFR for the chlorophyte archetypes was similar to that observed for several of the low-signal diatom archetypes, essentially background with little temporal variability. They will not be the focus of further discussion.

Multivariate analysis of normalized DNA RFR data was used to capture the temporal patterns in the RFR data, such that archetypes that covary in time are clustered together. The analysis identified two groups of archetypes and two individual archetypes (LEO212154 and PTRICORNUTUM) whose temporal patterns (variation, that is, increase or decrease with time, rather than absolute signal strength) were significantly different from each other (Figure 8a), as determined by a similarity profiles test. The two archetypes with distinct behavior were among those with the highest RFR, and archetypes within a second group, which included TOCEANICA, were characterized by widely varying magnitude of RFR but similar temporal patterns. The largest group of archetypes, which included MBAP19CONSENS, had generally low signals with little temporal variability.

Groupings of temporal patterns among archetypes differed markedly when cDNA RFR data were subjected to a similar analysis (Figure 8b). A nonparametric Mantel test based on the underlying resemblance matrices derived from DNA and cDNA RFR values indicates that the grouping in temporal patterns among archetypes are significantly related (Spearman's $r = 0.516$, $P = 0.003$). However, the correlation is not close to 1.0, and hence differences between patterns in abundance and expression of *NR* genes are important. In the analysis of cDNA, the archetype LEO212154 remained distinct from all others, but MBAP19CONSENS now grouped with TOCEANICA and TSTPSKENAS. PTRICORNUTUM grouped with MBAP22 and LEO212152. LEO21213 no longer grouped with TOCEANICA but with the larger grouping of generally low RFR archetypes, and CHLAMY was distinct from all other archetypes. In comparing Figures 6–8, it may be seen that the major archetypes, with highest RFR, separate out in the multidimensional scaling analysis because their peaks never coincided in time, as expected, but

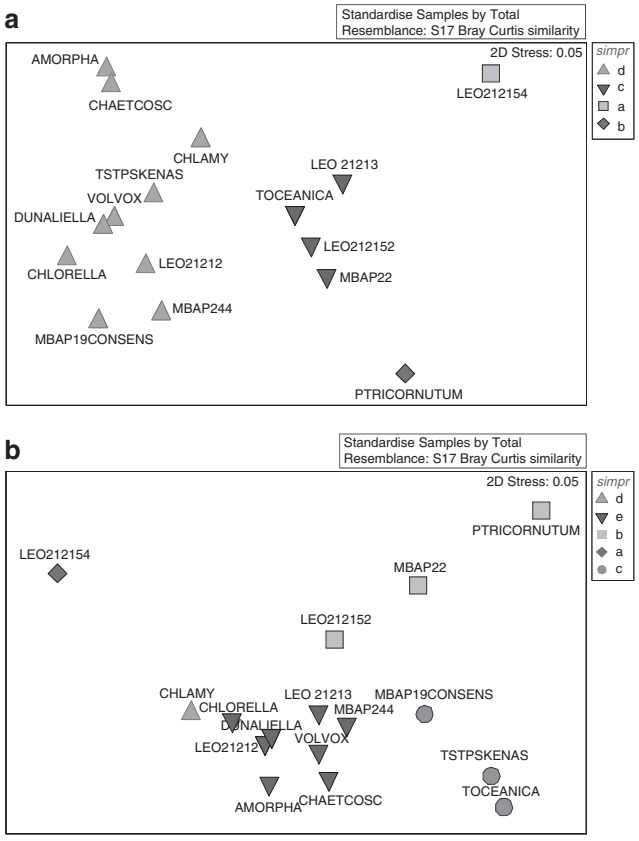

Figure 8 Two-dimensional nonmetric multidimensional scaling plots of RFR data for (**a**) DNA and (**b**) cDNA. Archetypes that showed similar temporal patterns (a hypothesis of no multivariate structure rejected at $P = 0.05$) are shown in the same color. A full color version of this figure is available at *The ISME Journal* online.

indicating variation in individual archetype response to environmental conditions.

Using multiple correlation analyses between normalized RFR and biogeochemical, hydrographic and uptake rate data, we found that TOCEANICA was positively correlated with NH_4^+ concentration ($R^2 = 0.761$, $P = 0.098$) and with the rate of ammonium uptake ($R^2 = 0.88$, $P = 0.026$) but not with any other variables (Supplementary Table 1). MBAP19-CONSENS was positively correlated with the uptake rates of both NO_3^- and NH_4^+ ($R^2 = 0.9$, $P = 0.013$). None of the other probes identified as distinct in the multidimensional scaling analysis, nor any of the clusters of probes, were significantly correlated with environmental or rate data.

Discussion

The seasonal patterns in temperature, leading to water column stratification, have been well described for this temperate region in the western English Channel (Southward *et al*., 2005). Stratification usually occurs in April, and the spring phytoplankton bloom follows causing nutrient depletion in the surface waters that extends through

until late September. This seasonal pattern was also seen during this study. However, as has been reported by Jordan and Joint (1998), there were also sporadic introductions of nutrients into the surface mixed layer, possibly as riverine input following rain events (see, for example, Rees *et al*., 2009), which were not in the Redfield ratio and which were quickly depleted. Jordan and Joint (1998) examined >1000 nitrate and phosphate measurements, obtained over a long time period (1930–1987), and found that the mean molar nitrate/phosphate ratio was only 11.6, much lower than the Redfield ratio of 16:1. Significantly, over that long time period, there were many transient increases in P that did not have equivalent increases in N. Interestingly, similar near-surface enrichments have also been reported for the North Pacific Ocean (Karl and Tien, 1992; Haury *et al*., 1994). However, the cause of these transients in nutrient concentration has not been adequately explained.

In the present study, there were also short-lived increases in some nutrient concentrations. Although we observed only very minor P transients, compared with those reported by Jordan and Joint (1998), there were occasions when changes in nutrient uptake kinetics implied that the phytoplankton populations were responding to sporadic nutrient inputs. In particular, a large increase in nitrate uptake was measured on 25 August, with a maximum in *f*-ratio, but there was only a small change detected in nitrate concentration; this was some weeks before nitrate concentrations returned to their winter maximum. However, the peak *f*-ratio was accompanied by a large change in silicate concentration, suggesting that silicate was not required at the same concentration as nitrate. Fucoxanthin concentrations were high in this sample, suggesting that diatoms were present in this late bloom. The dinoflagellate *Karenia* sp. (which contains some fucoxanthin) is often an important component of the late summer bloom in the western English Channel but was in decline on this date, having reached a maximum in the previous 2 weeks. Other dinoflagellates, mainly *Prorocentrum* sp. that typically do not contain fucoxanthin (Berden-Zrimec *et al*., 2008), were abundant in August. They may have contributed to the observed peak in nitrate assimilation, responding to increased nutrient supply by utilizing nitrate (and presumably phosphate) without a large requirement for silicate. In this case, because nutrient uptake rates were measured, we have been able to detect changes in phytoplankton activity that would not have been predicted from the observed variations in nutrient concentration, or from measures of phytoplankton abundance. It is clear that there can be very rapid variations in the supply of nutrients to the surface mixed layer in this region—and the phytoplankton populations respond very rapidly.

Although we have detailed information on phytoplankton species (from microscope and pigment analyses), it is difficult to draw convincing cause and effect conclusions from these standard biological oceanographic measurements. It is impossible to link specific phytoplankton species, or changes in apparent phytoplankton assemblage, to the observed variations in nutrient concentration or to nitrogen uptake rate measurements convincingly. For this reason, we investigated if species-specific *NR* abundance and expression might provide additional information that would lead to better understanding of phytoplankton–nutrient dynamics. Grazing on phytoplankton also plays a role in the seasonal patterns of population growth and assemblage composition, but less so in the specific phytoplankton–nutrient interactions that might be reflected in gene expression.

Significant correlations were detected between physical/chemical variables and a few of the archetypes (Supplementary Table 1). RFR for TOCEANICA and TSTPSKENAS cDNAs were negatively correlated with NO_3^- and NO_2^- concentrations, which may represent a phase phenomenon (higher relative biomass after the nutrients have been assimilated), whereas PTRICORNUTUM and TSTPSKENAS were positively correlated with temperature.

A few of the archetypes with largest RFR correlated with ammonium assimilation, either in the light or the dark. Although these archetypes all represent diatoms, which are often associated with nitrate uptake, their relative abundance in terms of *NR* archetypes was significantly related to ammonium uptake and not to nitrate uptake. The positive correlations between total chlorophyll and *f*-ratio, and between fucoxanthin and *f*-ratio (Figure 5), are consistent with greater importance of nitrate as an N source at higher biomass/productivity levels, but this simple correlation was not detected for most individual archetypes.

PTRICORNUTUM was the only archetype whose RFR was correlated with the *f*-ratio, and it was positively correlated at both DNA and RNA levels. Although the *f*-ratio was computed from Light minus Dark rates, PTRICORNUTUM was not correlated with absolute rate of nitrate uptake (Light minus Dark), although it was negatively correlated with the rate of ammonium uptake in the light. PTRICORNUTUM thus appears to exhibit a relationship with nitrogen uptake that is typically associated with diatoms, but which was not exhibited by other diatoms represented on the array.

Pearson correlation analysis using arcsin transformed RFR values for DNA and cDNA hybridization signals detected significant correlations among archetypes at both the DNA and cDNA levels that were consistent with the multidimensional scaling cluster analysis (Figures 8a and b). The composition of the clusters differed between DNA and cDNA and each of the archetypes with the largest RFR were in different clusters. These clusters represent archetypes that covary in time among the six dates and may identify ecologically important associations in terms of relative abundance and gene expression.

It was striking that none of the archetypes showed a significant correlation between cDNA and DNA when analyzed in a pairwise manner. Nonetheless, when grouped across all dates and all archetypes, cDNA and DNA RFR were significantly correlated ($R^2 = 0.610$, $P \ll 0.001$).

The lack of correlation between cDNA and DNA signals for individual archetypes could be because of differential regulation of NR in response to NO_3^- concentration and time of day. Gene regulation could result in gene expression varying much more rapidly than abundance, which could not be resolved with our sampling. The cDNA/DNA correlation for all archetypes suggests that despite variability among types, the most abundant types are the most active in gene expression, which is consistent with selection for growth of those types under favorable conditions.

The finding that two archetypes, MBAP19CONSENS and LEO212154, which were not associated with known diatom species, were among the strongest signals suggests that either these archetypes represent known species whose genes have not been sequenced or that abundant phylotypes are not represented in the culture collection. A screen of the GenBank database in April 2010 found that despite the presence of hundreds of additional *NR* sequences since the design of the original phytoarray, the original four *NR* sequences from New Jersey coastal waters upon which the LEO212154 probe was designed are still the only sequences with high identity to the probe. For MBAP19CONSENS, ~40 *NR* sequences were found that have high enough identities to hybridize with the probe. None of these represent cultivated species, and all of them were reported from two studies, one of seagrass epiphytes in Tampa Bay Florida (Adhitya *et al.*, 2007), and one a survey of *NR* and *rbcL* diversity in Monterey Bay and L4 phytoplankton assemblages (Bhadury and Ward, 2009).

The TOCEANICA probe has 100% identity only with itself, but has identity in the range of 87% with a number of environmental sequences obtained from the seagrass study (Adhitya *et al.*, 2007) as well as from Monterey Bay (Allen *et al.*, 2005). Sequences from *Skeletonema costatum*, *T. weissflogii* and *Asterionellopsis glacialis* are in the range of 85–87% identical, equivalent to the cutoff below which hybridization is negligible (Taroncher-Oldenburg *et al.*, 2003). *T. oceanica* was not individually enumerated in the L4 microscopy record, but it likely falls into the general categories '*Thalassiosira* 5, 10 and 20 μm', which were abundant during the summer bloom period (Widdicombe *et al.*, 2010).

P. tricornutum was not recorded in the microscopy data from L4 and we were initially skeptical that this species, known primarily as a laboratory model organism and usually isolated from nutrified or contaminated sites, could be an important component of the diatom assemblage of the western English Channel. The probe representing *P. tricornutum* is very specific, however, and there are no published sequences within 85% identity of the *P. tricornutum* *NR* sequence (all <80% identity). We are confident that these results do not result from contamination during DNA/RNA analysis. Negative controls in every PCR reaction ensured that no obvious contaminants were present in the targets prepared by PCR. It seems unlikely that seawater samples filtered in one lab and extracted in another could be contaminated by cultures growing elsewhere in the institution. Sterivex samples were extracted in different laboratories for DNA and RNA (Plymouth Marine Laboratory and Princeton University, respectively), and hence contamination would have had to be present in both locations. Thus, technical issues seem unlikely to account for the observations.

The explanation may be that *P. tricornutum* was present in the form of small oval-shaped cells, which would not have been recognized by microscopic inspection. *P. tricornutum* occurs in three shapes, the tricornered hat, the spindle and a small (3–8 μm diameter) oval (Allen *et al.*, 2008). The oval dominates most isolates when subjected to stress (De Martino *et al.*, 2007). Using a PCR assay designed to be specific for the intergenic transcribed spacer region of the *P. tricornutum* 18S rRNA genes, De Martino *et al.* (2007) detected *P. tricornutum* in the DNA extracts from April and July from which the array targets were prepared. In fact, one of the first isolations of a culture of *P. tricornutum*, then called *Nitzschia closterium var. minimutis*, was from the English Channel (Allen and Nelson, 1910). Thus, we conclude that the array detection of *P. tricornutum* was probably correct. Even 'known' species can be cryptic, illustrating the power of DNA/RNA-based detection methods.

The phytoarray demonstrates the potential to investigate the phytoplankton community assemblage at much higher resolution than can be accomplished with assays of total chlorophyll, ancillary pigments or cell counts. Even with the small number of archetype probes present on the array used here, differential temporal patterns were detected for multiple diatom types. The low-frequency array analysis reported here could be vastly improved upon with higher-frequency analysis, taking advantage of streamlined protocols developed recently. One of the interesting findings here is the relative importance (high RFR) of archetypes representing unknown organisms. It remains to be discovered whether these archetypes represent uncultivated types. Using probes derived from unknown types based on gene sequences retrieved from the environment, however, allows the detection of distinct temporal patterns and archetype associations that were not obvious from bulk measurements or cell counts.

The chemical and physical parameters over the time course showed the expected seasonal patterns, as did the overall general pattern of phytoplankton

biomass and N uptake rates. Simple correlations among overall abundances, archetype abundances, nutrient concentrations and chemical and physical parameters, however, were generally not significant and clearly did not describe the environmental responses of the phytoplankton. Observations of particular snapshots in time are not capable of identifying the processes responsible for patterns that result from previous conditions. Higher resolution time series of relative abundance and gene expression might make it possible to link past conditions with present patterns. Among all archetypes combined, RFR for cDNA and DNA patterns correlated, suggesting a general relationship between biomass and gene expression. However, on an individual basis, the correlations were weak and this mismatch may imply transitions in response to environmental conditions such as, for example, entering stationary phase or beginning of a growth phase. Higher temporal resolution in the array analysis and environmental sampling could link these processes to individual environmental stimuli.

Acknowledgements

We thank the staff of the Western English Channel Observatory and the crews of the research ships. Monitoring data are taken from the WEC Observatory database: nutrients measured by Malcolm Woodward, hydrographic data by Tim Smyth, phytoplankton counts by Derek Harbour (through 2004) and subsequently by Claire Widdicombe (beginning in 2005), and pigments by Carole Llewellyn. The microarray was printed by Donna Storton (Princeton University) and we gratefully acknowledge the Princeton University Microarray Facility. We thank the Natural Environment Research Council (UK) and the National Science Foundation (USA) for funding.

References

Adhitya A, Thomas FI, Ward BB. (2007). Diversity of assimilatory nitrate reductase genes from plankton and epiphytes associated with a seagrass bed. *Microb Ecol* **54**: 587–597.

Allen AE, LaRoche J, Maheswari U, Lommer M, Schauer N, Lopez PJ *et al*. (2008). Whole-cell response of the pennate diatom Phaeodactylum tricornutum to iron starvation. *Proc Natl Acad Sci USA* **105**: 10438–10443.

Allen AE, Ward BB, Song BK. (2005). Characterization of diatom (Bacillariophyceae) nitrate reductase genes and their detection in marine phytoplankton communities. *J Phycol* **41**: 95–104.

Allen EJ, Nelson EW. (1910). On the artificial culture of marine plankton organisms. *J Mar Biol Assoc UK* **8**: 421–474.

Berden-Zrimec M, Flander-Putrle V, Drinovec L, Zrimec A, Monti M. (2008). Growth, delayed fluorescence and pigment composition of four Prorocentrum minimum strains growing at two salinities. *Biol Res* **41**: 11–23.

Bhadury P, Ward BB. (2009). Molecular diversity of marine phytoplankton communities based on key functional genes. *J Phycol* **45**: 1335–1347.

Bulow SE, Francis CA, Jackson GA, Ward BB. (2008). Sediment denitrifier community composition and nirS gene expression investigated with functional gene microarrays. *Enviro Microbiol* **10**: 3057–3069.

Clarke KR, Gorley RN. (2006). *PRIMER v6: User Manual/ Tutorial*. Primer-E Ltd.: Plymouth, UK.

Clarke KR, Warwick RM. (2001). *Change in Marine Communities: An Approach to Statistical Analysis and Interpretation*, 2nd edn. Primer-E Ltd: Plymouth, UK.

Cooper LHN. (1937). On the ratio of nitrogen to phosphorus in the sea. *J Mar Biol Assoc UK* **22**: 177–182.

Cushing DH, Dickson RR. (1976). The biological response in the sea to climatic changes. *Adv Mar Biol* **14**: 2–122.

De Martino A, Meichenin A, Shi J, Pan KH, Bowler C. (2007). Genetic and phenotypic characterization of *Phaeodactylum tricornutum* (Bacillariophyceae) accessions. *J Phycol* **43**: 992–1009.

DeRisi J, Penland L, Brown PO, Bittner ML, Meltzer PS, Ray M *et al*. (1996). Use of a cDNA microarray to analyse gene expression patterns in human cancer. *Nat Genet* **14**: 457–460.

Dudley AM, Aach J, Steffen MA, Church GM. (2002). Measuring absolute expression with microarrays with a calibrated reference sample and an extended signal intensity range. *Proc Natl Acad Sci USA* **99**: 7554–7559.

Dugdale RC, Goering JJ. (1967). Uptake of new and regenerated forms of nitrogen in marine production. *Limnol Oceanogr* **12**: 196–206.

Eppley R. (1972). Temperature and phytoplankton growth in the sea. *Fish Bull, NOAA* **70**: 1063–1085.

Genner MJ, Halliday NC, Simpson SD, Southward AJ, Hawkins SJ, Sims DW. (2010). Temperature-driven phenological changes within a marine larval fish assemblage. *J Plankton Res* **32**: 699–708.

Gibb S, Mantoura RFC, Liss PS. (1995). Analysis of ammonia and methylamines in natural waters by flow injection gas diffusion coupled to ion chromatography. *Analytica Chimica Acta* **316**: 291–304.

Harris R. (2010). The L4 time series: the first 20 years. *J Plankton Res* **32**: 577–583.

Haury LR, Fey CL, Shulenberger E. (1994). Surface enrichment of inorganic nutrients in the North Pacific Ocean. *Deep-Sea Res Pt 1* **41**: 1191–1205.

Holmes RM, Aminor A, Kerouel R, Hooker BA, Peterson BJ. (1999). A simple and precise method for measuring ammonium in marine and freshwater ecosystems. *Can J Fish Aquat Sci* **56**: 1801–1808.

Joint I, Jordan MB, Carr MR. (1997). Is phosphate part of the Russell Cycle? *J Mar Biol Assoc UK* **77**: 625–634.

Joint IR, Jordan MB. (2008). The effect of short-term exposure to UVA and UVB on potential phytoplankton production in UK coastal waters. *J Plankton Res* **30**: 199–210.

Jordan MB, Joint I. (1998). Seasonal variation in nitrate, phosphate ratios in the English Channel 1923–1987. *Estuar Coast Shelf Sci* **46**: 157–164.

Karl DM, Tien G. (1992). MAGIC: a sensitive and precise method for measuring dissolved phosphorus in aquatic environments. *Limnol Oceanogr* **37**: 105–116.

Kovala PE, Larrance JD. (1966). Computation of phytoplankton cell numbers, cell volume, cell surface and plasma volume per litre, from microscopical counts. Special Report no. 38. Department of Oceanography, University of Washington.

Llewellyn C, Fishwick J, Blackford J. (2005). Phytoplankton community assemblage in the English Channel: a

comparison using chlorophyll a derived from HPLC-CHEMTAX and carbon derived from microscopy cell counts. *J Plankton Res* **27**: 103–119.

Matthews DJ. (1917). On the amount of phosphoric acid in the sea-water off Plymouth Sound II. *J Mar Biol Assoc UK* **11**: 251–257.

Menden-Deuer S, Lessard E. (2000). Carbon to volume relationships for dinoflagellates, diatoms, and other protist plankton. *Limnol Oceanogr* **45**: 569–579.

Redfield AC, Ketchum BH, Richards FA. (1963). The influence of organisms on the composition of sea water. In: Hill MN (ed.). *The Sea*. Wiley Interscience: New York, pp 26–77.

Rees AP, Hope S, Widdicombe CE, Dixon JL, Woodward EMS, Fitzsimmons JF. (2009). Alkaline phosphatase activity in the Western English Channel: elevations induced by high summer time rainfall. *Estuar Coast Shelf Sci* **81**: 569–574.

Rodriguez F, Fernandez E, Head R, Harbour D, Bratbak G, Heldal M *et al.* (2000). Temporal variability of viruses, bacteria, phytoplankton and zooplankton in the western English Channel off Plymouth. *J Mar Biol Assoc UK* **80**: 575–586.

Russell FR, Southward AJ, Boalch GT, Butler EI. (1971). Changes in biological conditions in the English Channel off Plymouth during the last half century. *Nature* **234**: 468–470.

Russell FS. (1936). The seasonal abundance of the pelagic young of teleostean fishes in the Plymouth area. Part III. The year 1935, with a note on the conditions as shown by the occurrence of plankton indicators. *J Mar Biol Assoc UK* **20**: 595–604.

Siddorn JR, Allen JI, Uncles RJ. (2003). Heat, salt and tracer transport in the Plymouth Sound coastal region: a 3-D modelling study. *J Mar Biol Assoc UK* **83**: 673–682.

Smyth TJ, Fishwick JR, Al-Moosawi L, Cummings DG, Harris C, Kitidis V *et al.* (2010). A broad spatio-temporal view of the Western English Channel observatory. *J Plankton Res* **32**: 585–601.

Southward AJ, Langmead O, Hardman-Mountford NJ, Aiken J, Boalch GT, Dando PR *et al.* (2005). Long-term oceanographic and ecological research in the Western English Channel. *Adv Mar Biol* **47**: 1–105.

Taroncher-Oldenburg G, Griner E, Francis CA, Ward BB. (2003). Oligonucleotide microarray for the study of functional gene diversity of the nitrogen cycle in the environment. *Appl Environ Microbiol* **69**: 1159–1171.

Throndsen J. (1978). Productivity and abundance of ultra-plankton and nanoplankton in Oslo Fjorden. *Sarsia* **63**: 273–284.

Ward BB. (2008). Phytoplankton community composition and gene expression of functional genes involved in carbon and nitrogen assimilation. *J Phycol* **44**: 1490–1503.

Widdicombe CE, Eloire D, Harbour D, Harris RP, Somerfield PJ. (2010). Long-term phytoplankton community dynamics in the Western English Channel. *J Plankton Res* **32**: 643–655.

Woodward EMS, Rees AP. (2001). Nutrient distributions in an anticyclonic eddy in the north east Atlantic Ocean, with reference to nanomolar ammonium concentrations. *Deep-Sea Res II* **48**: 775–793.

Wurmbach E, Yuen G, Sealfon SC. (2003). Focused microarray analysis. *Methods Enzymol* **31**: 306–316.

Supplementary Information accompanies the paper on The ISME Journal website (http://www.nature.com/ismej)